

# All-optical machine learning using diffractive deep neural networks

XING LIN , YAIR RIVENSON, NEZIH T. YARDIMCI , MUHAMMED VELI, [...], AND AYDOGAN OZCAN +2 authors [Authors Info & Affiliations](#)

SCIENCE 26 Jul 2018 Vol 361, Issue 6406 pp. 1004-1008 DOI: 10.1126/science.aat8084

79,965 downloads 1,782 citations

## All-optical deep learning

Deep learning uses multilayered artificial neural networks to learn digitally from large datasets. It then performs advanced identification and classification tasks. To date, these multilayered neural networks have been implemented on a computer. Lin *et al.* demonstrate all-optical machine learning that uses passive optical components that can be patterned and fabricated with 3D-printing. Their hardware approach comprises stacked layers of diffractive optical elements analogous to an artificial neural network that can be trained to execute complex functions at the speed of light.

Science, this issue p. [1004](#)

## Abstract

Deep learning has been transforming our ability to execute advanced inference tasks using computers. Here we introduce a physical mechanism to perform machine learning by demonstrating an all-optical diffractive deep neural network (D<sup>2</sup>NN) architecture that can implement various functions following the deep learning–based design of passive diffractive layers that work collectively. We created 3D-printed D<sup>2</sup>NNs that implement classification of images of handwritten digits and fashion products, as well as the function of an imaging lens at a terahertz spectrum. Our all-optical deep learning framework can perform, at the speed of light, various complex functions that computer-based neural networks can execute; will find applications in all-optical image analysis, feature detection, and object classification; and will also enable new camera designs and optical components that perform distinctive tasks using D<sup>2</sup>NNs.

### SIGN UP FOR THE AWARD-WINNING SCIENCEADVISER NEWSLETTER

The latest news, commentary, and research, free to your inbox daily

SIGN UP >

Deep learning is one of the fastest-growing machine learning methods ([1](#)). This approach uses multilayered artificial neural networks implemented in a computer to digitally learn data representation and abstraction and to perform advanced tasks in a manner comparable or even superior to the performance of human experts. Recent examples in which deep learning has made major advances in machine learning include medical image analysis ([2](#)), speech recognition ([3](#)), language translation ([4](#)), and image classification ([5](#)), among others ([1](#), [6](#)). Beyond some of these mainstream applications, deep learning methods are also being used to solve inverse imaging problems ([7–13](#)).

ScienceAdviser

Get Science’s award-winning newsletter with the latest news, commentary, and research, free to your inbox daily.

SUBSCRIBE

NOT NOW

amplitude and phase of which are determined by the product of the input wave and the complex-valued transmission or reflection coefficient at that point [see (14) for an analysis of the waves within a D<sup>2</sup>NN]. Therefore, an artificial neuron in a D<sup>2</sup>NN is connected to other neurons of the following layer through a secondary wave modulated in amplitude and phase by both the input interference pattern created by the earlier layers and the local transmission or reflection coefficient at that point. As an analogy to standard deep neural networks (Fig. 1D), one can consider the transmission or reflection coefficient of each point or neuron as a multiplicative “bias” term, which is a learnable network parameter that is iteratively adjusted during the training process of the diffractive network, using an error back-propagation method. After this numerical training phase, the D<sup>2</sup>NN design is fixed and the transmission or reflection coefficients of the neurons of all layers are determined. This D<sup>2</sup>NN design—once physically fabricated using techniques such as 3D-printing or lithography—can then perform, at the speed of light, the specific task for which it is trained, using only optical diffraction and passive optical components or layers that do not need power, thereby creating an efficient and fast way of implementing machine learning tasks.

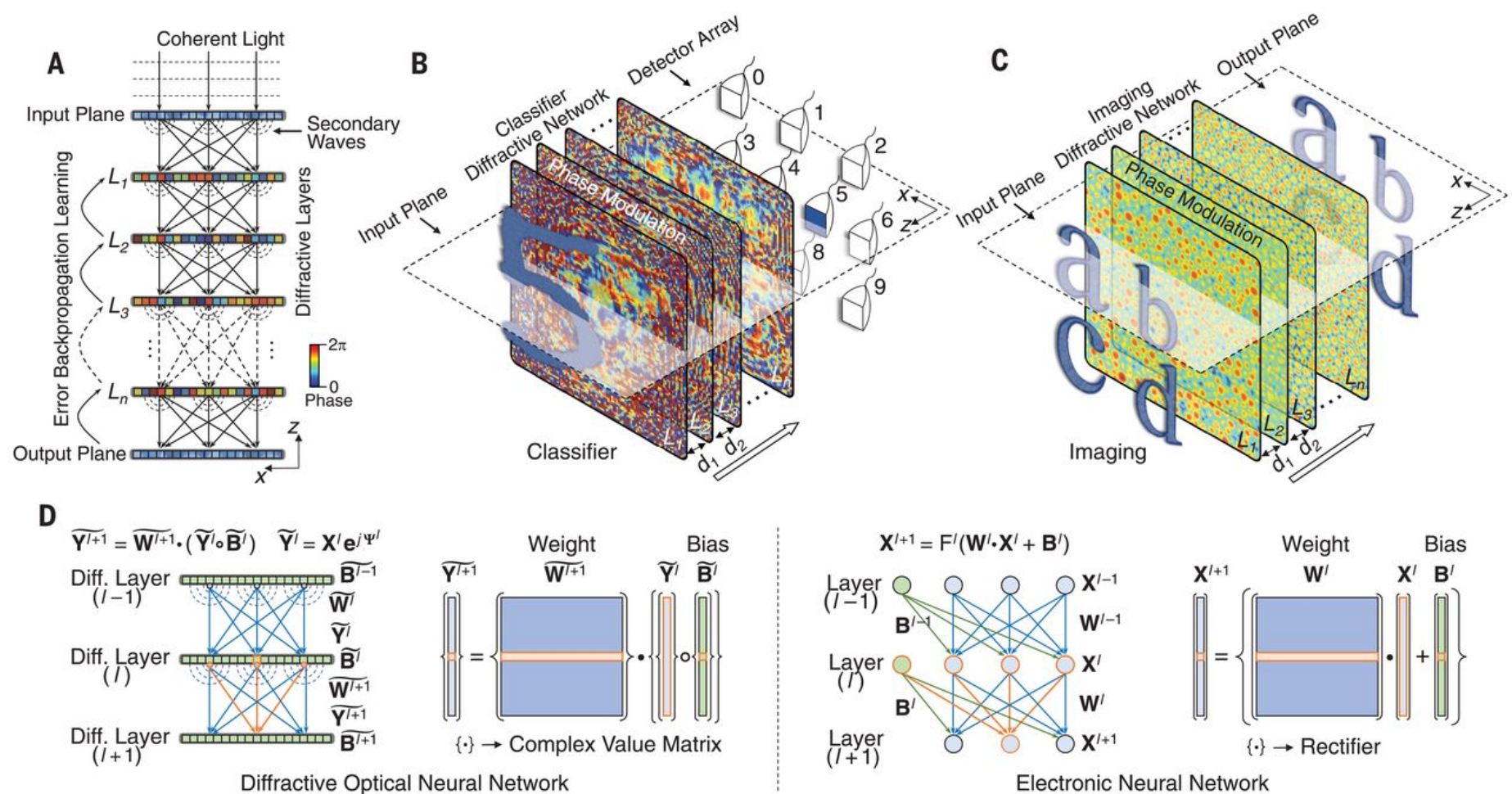


**Fig. 1 Diffractive deep neural networks (D<sup>2</sup>NNs).**

(A) A D<sup>2</sup>NN comprises multiple transmissive (or reflective) layers, where each point on a given layer acts as a neuron, with a complex-valued transmission (or reflection) coefficient. The transmission or reflection coefficients of each layer can be trained by using deep learning to perform a function between the input and output planes of the network. After this learning phase, the D<sup>2</sup>NN design is fixed; once fabricated or 3D-printed, it performs the learned function at the speed of light.  $L$ , layer. (B and C) We trained and experimentally implemented different types of D<sup>2</sup>NNs: (B) classifier (for handwritten digits and fashion products) and (C) imager.  $d$ , distance. (D) Comparison between a D<sup>2</sup>NN and a conventional neural network (14). Based on coherent waves, the D<sup>2</sup>NN operates on complex-valued inputs, with multiplicative bias terms. Weights in a D<sup>2</sup>NN are based on free-space diffraction and determine the interference of the secondary waves that are phase- and/or amplitude-modulated by the previous layers. “ $\circ$ ” denotes a Hadamard product operation. “Electronic neural network” refers to the conventional neural network virtually implemented in a computer.  $\mathbf{Y}$ , optical field at a given layer;  $\psi$ , phase of the optical field;  $\mathbf{X}$ , amplitude of the optical field;  $F$ , nonlinear rectifier function [see (14) for a discussion of optical nonlinearity in D<sup>2</sup>NN].

In general, the phase and amplitude of each neuron can be learnable parameters, providing a complex-valued modulation at each layer, which improves the inference performance of the diffractive network (fig. S1) (14). For coherent transmissive networks with phase-only modulation, each layer can be approximated as a thin optical element (Fig. 1). Through deep learning, the phase values of the neurons of each layer of the diffractive network are iteratively adjusted (trained) to perform a specific function by feeding training data at the input layer and then computing the network’s output through optical diffraction. On the basis of the calculated error with respect to the target output, determined by the desired function, the network structure and its neuron phase values are optimized via an error back-propagation algorithm, which is based on the stochastic gradient descent approach used in conventional deep learning (14).

To demonstrate the performance of the D<sup>2</sup>NN framework, we first trained it as a digit classifier to perform automated classifica-

**ScienceAdviser**

Get Science’s award-winning newsletter with the latest news, commentary, and research, free to your inbox daily.

SUBSCRIBE

NOT NOW



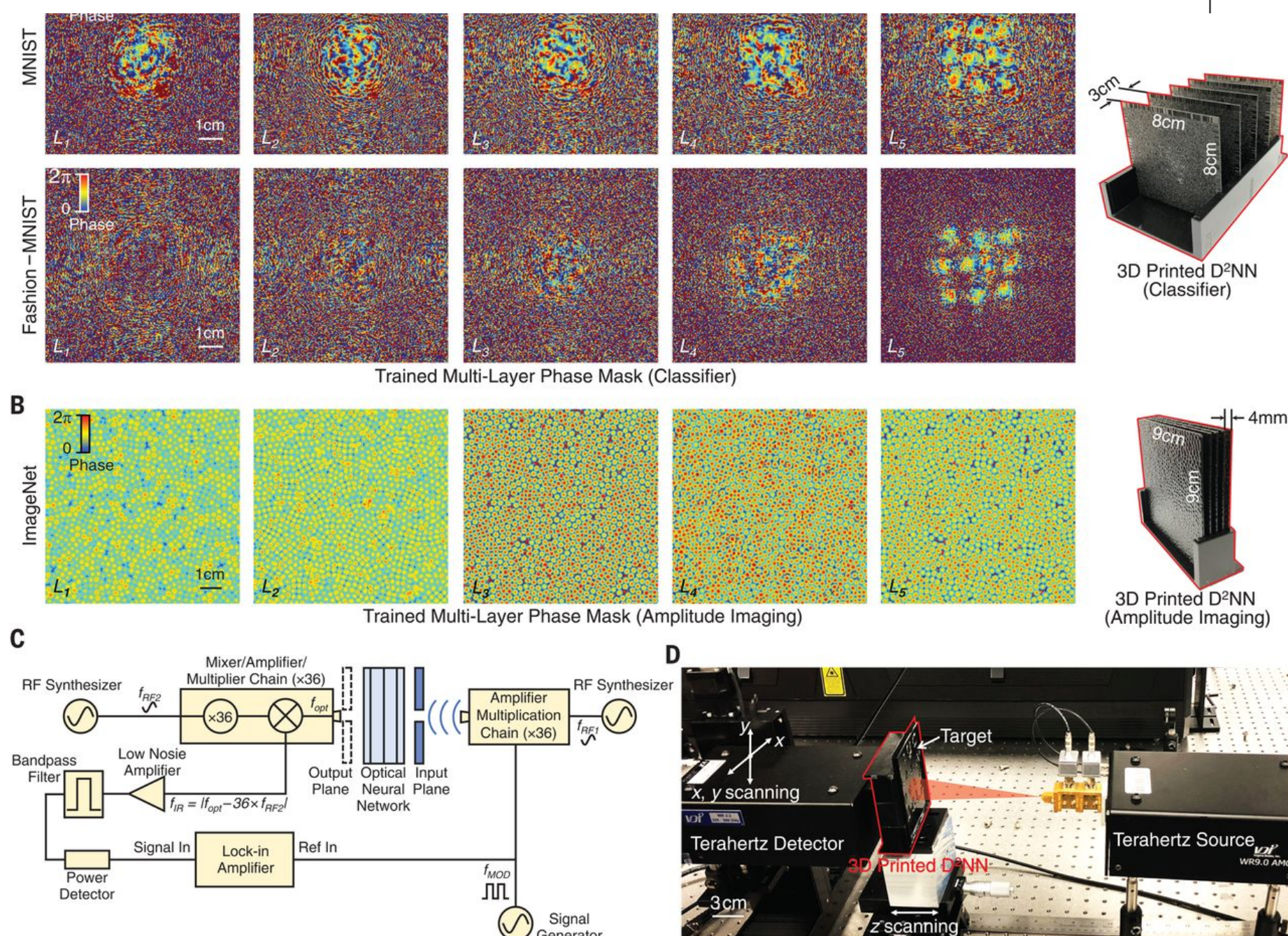


**Fig. 2 Experimental testing of 3D-printed D<sup>2</sup>NNs.**

(**A** and **B**) After the training phase, the final designs of five different layers ( $L_1, L_2, \dots, L_5$ ) of the handwritten digit classifier, fashion product classifier, and the imager D<sup>2</sup>NNs are shown. To the right of the network layers, an illustration of the corresponding 3D-printed D<sup>2</sup>NN is shown. (**C** and **D**) Schematic (**C**) and photo (**D**) of the experimental terahertz setup. An amplifier-multiplier chain was used to generate continuous-wave radiation at 0.4 THz, and a mixer-amplifier-multiplier chain was used for the detection at the output plane of the network. RF, radio frequency;  $f$ , frequency.

After training, the design of the D<sup>2</sup>NN digit classifier was numerically tested using 10,000 images from the MNIST test dataset (which were not used as part of the training or validation image sets) and achieved a classification accuracy of 91.75% (Fig. 3C and fig. S1). In addition to the classification performance of the diffractive network, we also analyzed the energy distribution observed at the network output plane for the same 10,000 test digits (Fig. 3C), the results of which clearly demonstrate that the diffractive network learned to focus the input energy of each handwritten digit into the correct (i.e., the target) detector region, in accord with its training. With the use of complex-valued modulation and increasing numbers of layers, neurons, and connections in the diffractive network, our classification accuracy can be further improved (figs. S1 and S2). For example, fig. S2 demonstrates a Lego-like physical transfer learning behavior for D<sup>2</sup>NN framework, where the inference performance of an already existing D<sup>2</sup>NN can be further improved by adding new diffractive layers—or, in some cases, by peeling off (i.e., discarding) some of the existing layers—where the new layers to be added are trained for improved inference (coming from the entire diffractive network: old and new layers). By using a patch of two layers added to an existing and fixed D<sup>2</sup>NN design ( $N = 5$  layers), we improved our MNIST classification accuracy to 93.39% (fig. S2) (14); the state-of-the-art convolutional neural network performance has been reported as 99.60 to 99.77% (16–18). More discussion on reconfiguring D<sup>2</sup>NN designs is provided in the supplementary materials (14).



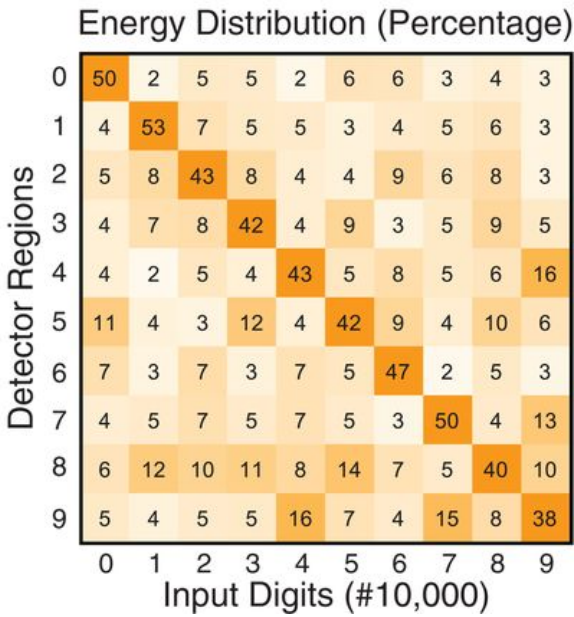
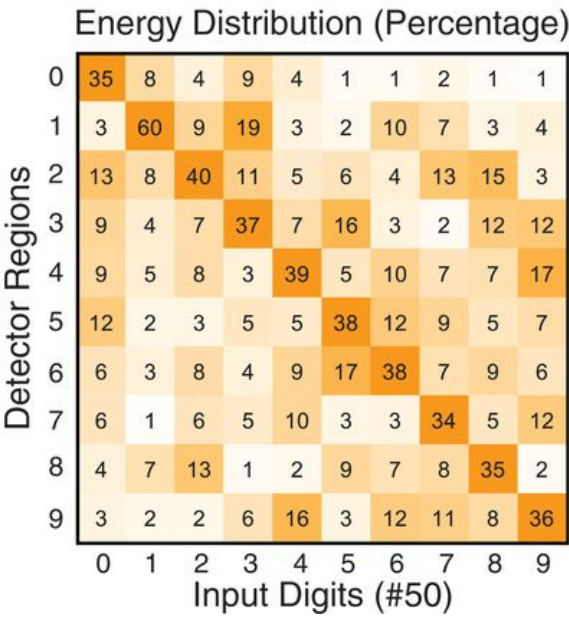
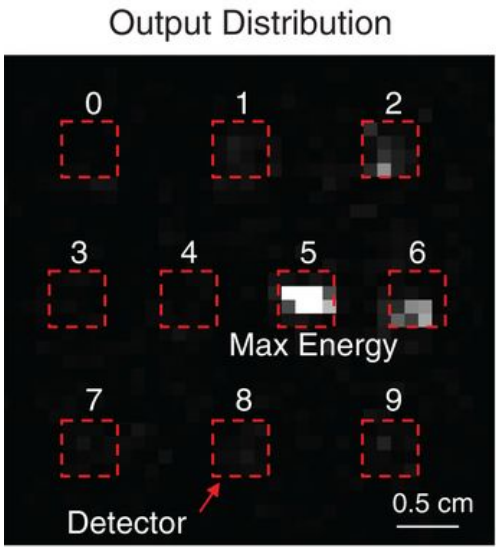
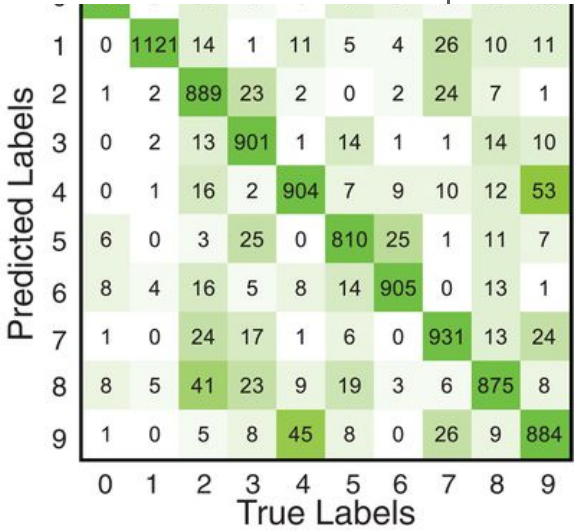
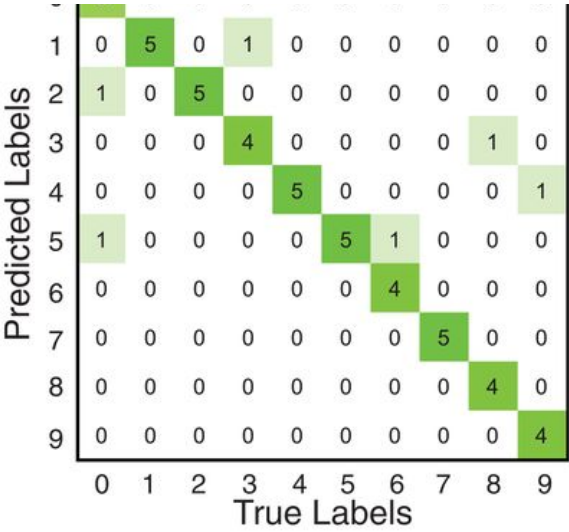
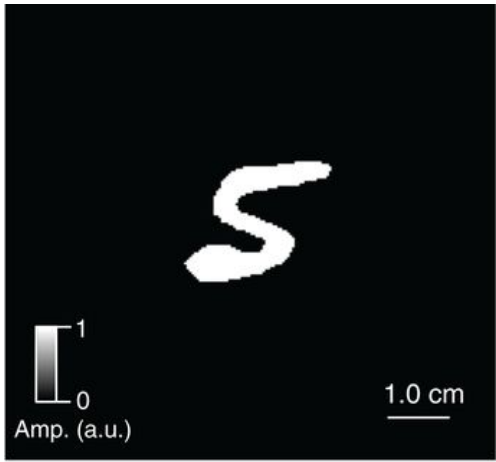


**Fig. 3 Handwritten digit classifier D<sup>2</sup>NN.** (A) A 3D-printed D<sup>2</sup>NN successfully classifies handwritten input digits (0, 1, ..., 9) on the basis of 10 different detector regions at the output plane of the network, each corresponding to one digit. As an example, the output image of the 3D-printed D<sup>2</sup>NN for a handwritten input of “5” is demonstrated, where the red dashed squares represent the trained detector regions for each digit. Other examples of our experimental results are shown in fig. S9. (B) Confusion matrix and energy distribution percentage for our experimental results, using 50 different handwritten digits (five for each digit) that were 3D-printed, selected among the images for which numerical testing was successful. (C) Same as (B), except summarizing our numerical testing results for 10,000 different handwritten digits (~1000 for each digit), achieving a classification accuracy of 91.75% using a five-layer design. Our classification accuracy increased to 93.39% by increasing the number of diffractive layers to seven, using a patch of two additional diffractive layers added to an existing and fixed D<sup>2</sup>NN (fig. S2).

Following these numerical results, we 3D-printed our five-layer D<sup>2</sup>NN design (Fig. 2A), with each layer having an area of 8 cm by 8 cm, followed by 10 detector regions defined at the output plane of the diffractive network (Figs. 1B and 3A). We then used continuous-wave illumination at 0.4 THz to test the network’s inference performance (Figs. 2, C and D). Phase values of each layer’s neurons were physically encoded using the relative thickness of each 3D-printed neuron. Numerical testing of this five-layer D<sup>2</sup>NN design achieved a classification accuracy of 91.75% over ~10,000 test images (Fig. 3C). To quantify the match between these numerical testing results and our experiments, we 3D-printed 50 handwritten digits (five different inputs per digit), selected among the same 91.75% of the test images for which numerical testing was successful. For each input object that is uniformly illuminated with the terahertz source, we imaged the output plane of the D<sup>2</sup>NN to map the intensity distribution for each detector region that is assigned to a digit. The results (Fig. 3B) demonstrate the success of the 3D-printed diffractive neural network and its inference capability: The average intensity distribution at the output plane of the network for each input digit clearly reveals that the 3D-printed D<sup>2</sup>NN was able to focus the input energy of the beam and achieve a maximum signal at the corresponding detector region assigned for that digit. Despite 3D-printing errors, possible alignment issues, and other experimental error sources in our setup (14), the match between the experimental and numerical testing of our five-layer D<sup>2</sup>NN design was found to be 88% (Fig. 3B). This relatively small reduction in the performance of the experimental network compared to our numerical test-

Next, we tested the classification performance of D<sup>2</sup>NN framework with a more complicated image dataset—i.e., the Fashion-MNIST dataset (19), which includes 10 classes, each representing a fashion product (t-shirts, trousers, pullovers, dresses, coats, sandals, shirts, sneakers, bags, and ankle boots; see fig. S3 for sample images). In general, for a coherently illuminated D<sup>2</sup>NN, we

ScienceAdviser

Get Science’s award-winning newsletter with the latest news, commentary, and research, free to your inbox daily.

SUBSCRIBE NOT NOW



...ational neural net-based standard deep learning, the state-of-the-art performance for Fashion-MNIST classification accuracy, has been reported as 96.7%, using ~8.9 million learnable parameters and ~2.5 million neurons (20).

To experimentally demonstrate the performance of fashion product classification using a physical D<sup>2</sup>NN, we 3D-printed our phase-only five-layer design and 50 fashion products used as test objects (five per class) on the basis of the same procedures employed for the digit classification diffractive network (Figs. 2A and 3), except that each input object information was encoded in the phase channel. Our results are summarized in Fig. 4, revealing a 90% match between the experimental and numerical testing of our five-layer D<sup>2</sup>NN design, with five errors out of 50 fashion products. Compared with digit classification (six errors out of 50 digits; Fig. 3), this experiment yielded a slightly better match between the experimental and numerical testing results (despite the more challenging nature of Fashion-MNIST dataset), perhaps because we used the phase channel, which does not suffer from the challenges associated with 3D-printing of void regions [such as in digits 0, 6, 8, and 9 (Fig. 3)], to encode input image information for fashion products.

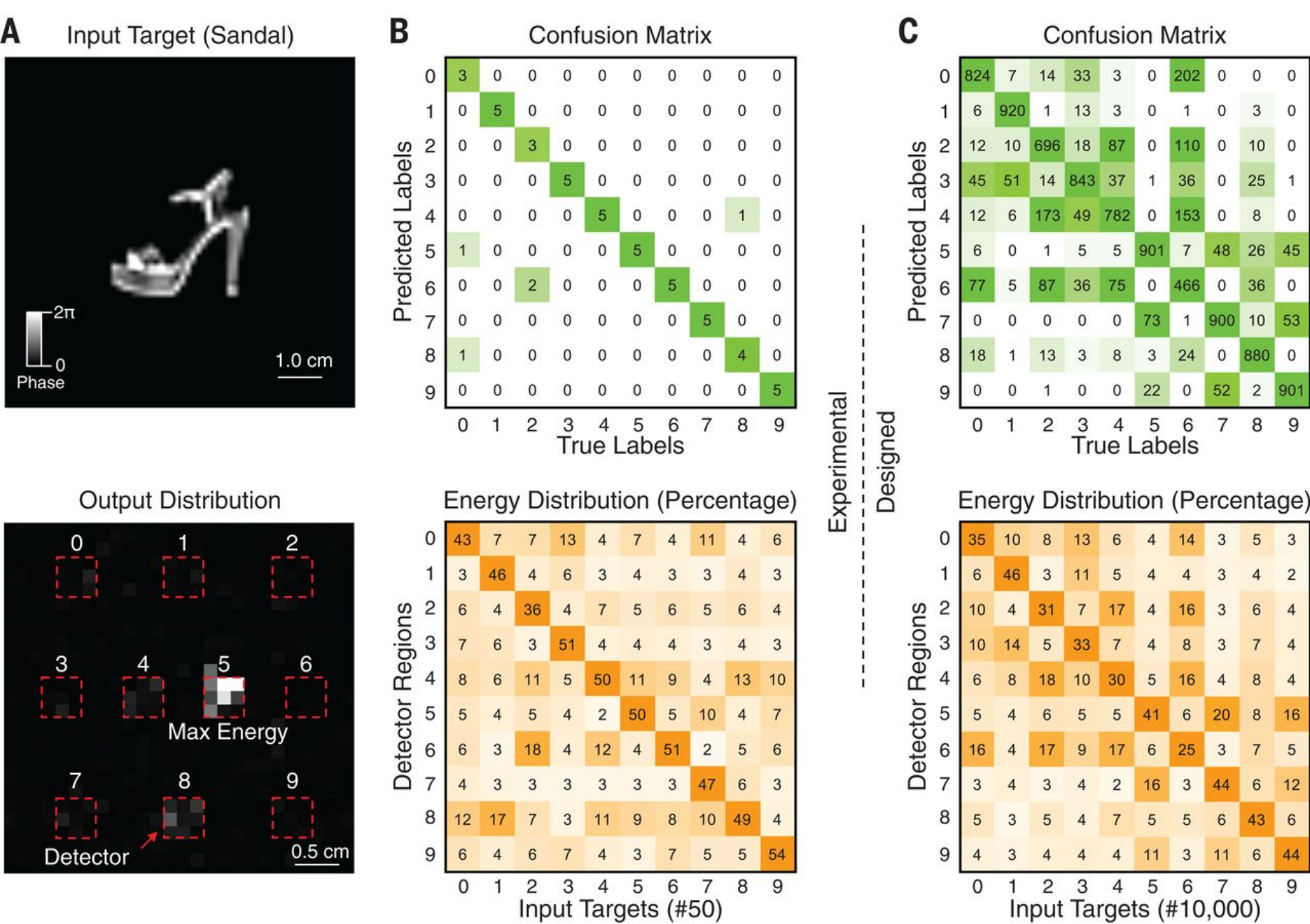


**Fig. 4 Fashion product classifier D<sup>2</sup>NN.** (A) As an example, the output image of the 3D-printed D<sup>2</sup>NN for a sandal input (Fashion-MNIST class 5) is demonstrated. The red dashed squares represent the trained detector regions for each fashion product. Other examples of our experimental results are shown in fig. S10. (B) Confusion matrix and energy distribution percentage for our experimental results, using 50 different fashion products (five per class) that were 3D-printed, selected among the images for which numerical testing was successful. (C) Same as (B), except summarizing our numerical testing results for 10,000 different fashion products (~1000 per class), achieving a classification accuracy of 81.13% using a five-layer design. By increasing the number of diffractive layers to 10, our classification accuracy increased to 86.60% (fig. S5).

Next, we tested the performance of a phase-only D<sup>2</sup>NN, composed of five 3D-printed transmission layers to implement amplitude imaging (Fig. 2B). This network was trained using the ImageNet database (21) to create a unit-magnification image of the input optical field amplitude at its output plane (~9 cm by 9 cm)—that is, the output image has the same physical size as the input object (14). As illustrated in fig. S6, A and C, the trained network initially connects every amplitude point at the input plane to various neurons and features of the following layers, which then focus the light back to a point at the output (i.e., image) plane, which is, as expected, quite different than the case of free-space diffraction (i.e., without the presence of the diffractive network),

in output images, each with a full width at half maximum of 1.0, 1.1, and 2.0 mm, respectively (fig. S6B). Our results also revealed that the printed network can resolve a linewidth of 1.8 mm at 0.4 THz (corresponding to a wavelength of 0.75 mm in air), which is slightly worse in resolution compared with the numerical testing of our D<sup>2</sup>NN design, where the network could resolve a linewidth of ~1.2 mm (fig. S7C). This experimental degradation in the performance of the diffractive network can be due to factors such as 3D-printing errors, potential misalignments, and absorption-related losses in the 3D-printed network ([14](#)).

Optical implementation of machine learning in artificial neural networks is promising because of the parallel computing capability and power efficiency of optical systems ([22–24](#)). Compared with previous optoelectronics-based learning approaches ([22, 25–27](#)), the D<sup>2</sup>NN framework provides a distinctive all-optical machine learning engine that efficiently operates at the speed of light using passive components and optical diffraction. An important advantage of D<sup>2</sup>NNs is that they can be easily scaled up using various high-throughput and large-area 3D-fabrication methods (such as soft lithography and additive manufacturing), as well as wide-field optical components and detection systems, to cost-effectively reach tens to hundreds of millions of neurons and hundreds of billions of connections in a scalable and power-efficient manner. For example, integration of D<sup>2</sup>NNs with lensfree on-chip imaging systems ([28, 29](#)) could provide extreme parallelism within a cost-effective and portable platform. Such large-scale D<sup>2</sup>NNs may be transformative for various applications, including image analysis, feature detection, and object classification, and may also enable new microscope or camera designs that can perform specific imaging tasks using D<sup>2</sup>NNs. To achieve these new technologies, nonlinear optical materials ([14](#)) and a monolithic D<sup>2</sup>NN design that combines all layers of the network as part of a 3D-fabrication method would be desirable. Among other techniques, laser lithography based on two-photon polymerization ([30](#)) can provide solutions for creating such D<sup>2</sup>NNs.

## Acknowledgments

We thank D. Mengu, Z. Wei, X. Wang, and Y. Xiao of UCLA for assistance with coding. **Funding:** The Ozcan Group at UCLA acknowledges the support of the National Science Foundation and the Howard Hughes Medical Institute. **Author contributions:** A.O., X.L., and Y.R. conceived of the research; X.L., N.T.Y., Y.L., Y.R., M.V., and M.J. contributed to the experiments; X.L., N.T.Y., M.V., and Y.R. processed the data; A.O., X.L., M.V., N.T.Y., Y.R., Y.L., and M.J. prepared the manuscript; and A.O. initiated and supervised the research. **Competing interests:** A.O., X.L., and Y.R. are inventors of a patent application on D<sup>2</sup>NNs. **Data and materials availability:** All data and methods are present in the main text and supplementary materials.

## Supplementary Material

### Summary

Materials and Methods

Figs. S1 to S16

References ([31–46](#))

### Resources

File (aat8084-lin-sm-rev-3.pdf)

DOWNLOAD

5.87 MB

File (aat8084-lin-sm.pdf)

DOWNLOAD

5.68 MB

ScienceAdviser

Get *Science's* award-winning newsletter with the latest news, commentary, and research, free to your inbox daily.

SUBSCRIBE

NOT NOW

SHOW ALL REFERENCES

eLetters (1)

eLetters is a forum for ongoing peer review. eLetters are not edited, proofread, or indexed, but they are screened. eLetters should provide substantive and scholarly commentary on the article. Neither embedded figures nor equations with special characters can be submitted, and we discourage the use of figures and equations within eLetters in general. If a figure or equation is essential, please include within the text of the eLetter a link to the figure, equation, or full text with special characters at a public repository with versioning, such as Zenodo. Please read our [Terms of Service](#) before submitting an eLetter.

LOG IN TO SUBMIT A RESPONSE

NOV. 23, 2018

A "diffractive deep neural network" is NOT an all-optical implementation of a conventional deep neural network

HAIQING WEI Scientist, Ambow Research Institute  
GANG HUANG Scientist, Ambow Research Institute  
XIUQING WEI Professor, The Third Affiliated Hospital of Sun Yat-sen University  
YANLONG SUN Professor, Texas A&M University  
HONGBIN WANG Professor, Texas A&M University

Here Lin et al. report a remarkable proposal that employs a passive, strictly linear optical setup to perform pattern classifications. But readers are strongly advised to draw a clear distinction between the so-called "diffractive deep neural network" (D2NN) and an all-optical implementation of a deep neural network (DNN) in the canonical sense. While the purported...

[view more](#)

Recommended articles from TrendMD

- Experimentally realized in situ backpropagation for deep learning in photonic neural networks  
Sunil Pai, Science, 2023
- This Week in Science  
Ian S. Osborne, Science, 2018
- Backpropagation-free training of deep physical neural networks  
Ali Momeni, Science, 2023
- Delocalized photonic deep learning on the internet’s edge  
Alexander Sludds, Science, 2022
- Geometric deep optical sensing  
Shaofan Yuan, Science, 2023

- Accelerating spin Hall conductivity predictions via machine learning [↗](#)  
Jinbin Zhao, Materials Genome Engineering Advances, 2024
- Employing deep learning in non-parametric inverse visualization of elastic–plastic mechanisms in dual-phase steels [↗](#)  
Siyu Han, Materials Genome Engineering Advances, 2024
- Artificial Intelligence & Medical Imaging Collection of Precision Clinical Medicine [↗](#)  
Precision Clinical Medicine, 2024
- A review on the applications of graph neural networks in materials science at the atomic scale [↗](#)  
Xingyue Shi, Materials Genome Engineering Advances, 2024
- A machine learning-based crystal graph network and its application in development of functional materials [↗](#)  
Gang Xu, Materials Genome Engineering Advances, 2024

ScienceAdviser

Get Science’s award-winning newsletter with the latest news, commentary, and research, free to your inbox daily.

SUBSCRIBE

NOT NOW



CURRENT ISSUE



There are no results at this time

Sign up for ScienceAdviser

Get *Science*’s award-winning newsletter with the latest news, commentary, and research, free to your inbox daily.

SUBSCRIBE >

LATEST NEWS

NEWS | 2 OCT 2025  
Could technology reduce fractures in racehorses?

SCIENCEINSIDER | 2 OCT 2025  
After months in limbo, four NIH institute directors fired

NEWS | 1 OCT 2025  
Wildfire smoke is charring your wine. This microbe could help

SCIENCEINSIDER | 1 OCT 2025  
AI reveals vast ‘ghost forests’ along U.S. coast

NEWS | 1 OCT 2025  
China launches ambitious collaboration to map primate brains—including ours

NEWS | 1 OCT 2025  
Ancient DNA from horses slaughtered by Neanderthals sheds light on equine evolution

RECOMMENDED

RESEARCH ARTICLE | MARCH 2024  
Mechanism for feature learning in neural networks and backpropagation-free machine learning models

RESEARCH ARTICLE | MARCH 2021  
Spectrally encoded single-pixel machine vision using diffractive networks

REPORTS | JULY 2006  
Reducing the Dimensionality of Data with Neural Networks

RESEARCH ARTICLE | JUNE 2022  
All-optical graph representation learning using integrated diffractive photonic computing units

SPONSORED WEBINAR | TECHNOLOGY | 3 OCT 2025  
From lab to marketplace: Turning research into real-world impact

ScienceAdviser

Get *Science*’s award-winning newsletter with the latest news, commentary, and research, free to your inbox daily.

SUBSCRIBE

NOT NOW



## AUTHORS & REVIEWERS

[Information for Authors](#)

[Information for Reviewers](#)

HELP

[FAQs](#)

[Access and Subscriptions](#)

[Order a Single Issue](#)

[Reprints and Permissions](#)

[TOC Alerts and RSS Feeds](#)

[Contact Us](#)

[Terms of Service](#) | [Privacy Policy](#) | [Accessibility](#)

**NOT NOW**